

## Analysis of Mutational Lesions of Acetate Metabolism in *Neurospora crassa* by $^{13}\text{C}$ Nuclear Magnetic Resonance

GRAHAM H. THOMAS<sup>1†</sup> AND ROBERT L. BAXTER<sup>2\*</sup>

*Department of Genetics, University of Edinburgh, Edinburgh, EH9 3JN,<sup>1</sup> and Department of Chemistry, University of Edinburgh, Edinburgh, EH9 3JJ,<sup>2</sup> United Kingdom*

Received 24 January 1986/Accepted 18 August 1986

The adaptation of *Neurospora crassa* mycelium to growth on acetate as the sole carbon source was examined by using  $^{13}\text{C}$  nuclear magnetic resonance. Extracts were examined by nuclear magnetic resonance at various times after transfer of the mycelium from medium containing sucrose to medium containing [ $2\text{-}^{13}\text{C}$ ]acetate as the sole carbon source. The label was initially seen to enter the alanine, glutamate, and glutamine pools, and after 6 h  $^{13}\text{C}$ -enriched trehalose was evident, indicating that gluconeogenesis was occurring. Analysis of the isotopomer ratios in the alanine and glutamate-glutamine pools indicated that substantial glyoxylate cycle activity became evident between 2 and 4 h after transfer. Immediately after transfer of the mycelium to acetate medium, the alanine pool increased to about four times its previous level, only a small fraction of which was enriched with  $^{13}\text{C}$ . The quantity of  $^{13}\text{C}$ -enriched alanine remained almost constant between 2 and 7.5 h after the transfer, whereas the overall alanine pool decreased to its original level. The selective catabolism of the unenriched alanine leads us to suggest that the alanine pool is partitioned into two compartments during adaptation. Two acetate-nonutilizing mutants were also studied by this technique. An *acu-3* strain, deficient for isocitrate lyase (EC 4.1.3.1) activity, showed metabolic changes consistent with this lesion. An *acp* strain, previously thought to be deficient in an inducible acetate permease, took up [ $2\text{-}^{13}\text{C}$ ]acetate but showed no evidence of glyoxylate cycle activity despite synthesizing the necessary enzymes; the lesion was therefore reinterpreted.

*Neurospora crassa* shares with many other organisms the ability to use both carbohydrates and acetate or acetogenic precursors such as higher fatty acids as carbon sources for growth (5). In the latter case, the carbon is assimilated via acetyl coenzyme A (CoA) into the glyoxylate cycle, which can be considered both as an anaplerotic pathway for the tricarboxylic acid (TCA) cycle and as a biosynthetic pathway for the synthesis of gluconeogenic precursors (5). In many eucaryotes, glyoxylate cycle activity is associated with a unique organelle called the glyoxysome (4, 5). However, there is considerable variation in the degree of autonomy of glyoxysome function among different species. In the castor bean endosperm, isozymes for the reactions common to both the TCA and glyoxylate cycles are present in the glyoxysome (4), but in *N. crassa* the glyoxysome has been shown to contain only the enzymes isocitrate lyase (EC 4.1.3.1), malate synthase (EC 4.1.3.2), and a variable proportion of the malate dehydrogenase (EC 4.1.1.40) of the cell (18). Citrate synthase (EC 4.1.3.7), succinate dehydrogenase (EC 1.3.99.1), and the NAD- and NADP-linked isocitrate dehydrogenases (EC 1.1.1.41 and EC 1.1.1.42, respectively) are restricted to the mitochondrion (25). This implies that in *N. crassa*, there must be close metabolic cooperation between the two organelles during growth on acetate. The essential features of the precursor-product relationships are shown schematically in Fig. 1.

The genes specifying the enzymes acetyl-CoA synthetase (EC 6.2.1.1), isocitrate lyase, malate synthase, and phosphoenolpyruvate (PEP) carboxykinase (EC 4.1.1.32), which are necessary for growth on exogenous acetate, are not expressed to any significant extent during growth on

carbohydrates. When acetate is substituted for sugars as the sole carbon source, these genes are induced or derepressed or both (11, 12). The transition from glycolytic to glyoxylate metabolism has been shown to involve significant changes in the specific activities of other enzymes common to the glyoxylate and TCA cycles, notably, increases in the activity of citrate synthase, malate dehydrogenase, and NADP-linked isocitrate and glutamate dehydrogenases together with a decrease in the activity of NAD-linked glutamate dehydrogenase (11). Some indication of the relative importance of these changes in metabolic activity to the ability of the fungus to grow on acetate has been gained from enzyme activity measurements and complementation studies with mutants of *N. crassa* which lack the ability to use acetate as the sole carbon source (*acu* mutants) (10). Although the evidence from in vitro enzyme analyses with wild-type and mutant strains suggests that a coordinated adaptation of metabolic activity is involved in the switch from glycolytic to acetate growth, no detailed information on the effects of these changes on metabolism in vivo is available.

$^{13}\text{C}$  nuclear magnetic resonance (NMR) spectroscopy is a particularly powerful tool for the investigation of cellular metabolism since it allows simultaneous measurement of the incorporation of label into specific carbons of a large number of metabolites (2, 3). Furthermore, analysis of  $^{13}\text{C}$ - $^{13}\text{C}$  coupling data, available from high-resolution spectra, provides a means of quantifying the proportions of individual isotopically enriched species (isotopomers) in a mixture and hence estimation of the contributions of different pathways to the synthesis of a metabolite (8, 21, 22). This approach has been successfully applied in investigations of the metabolism of acetate in acetate-adapted (6) and sporulating (8) *Saccharomyces cerevisiae* cells.

Both  $^{31}\text{P}$  and  $^{13}\text{C}$  NMR methods have been used for the characterization of glycolysis pathway mutants of *S. cerevi-*

\* Corresponding author.

† Present address: Department of Biology, Washington University, St. Louis, MO 63130.

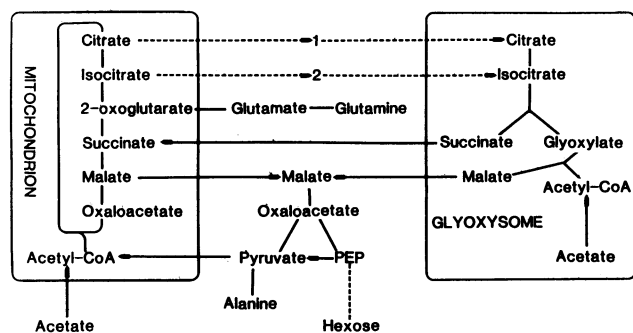


FIG. 1. Proposed metabolic network for biochemical inter-conversions observed in this study. Pathways 1 and 2 are possible routes for carbon to be supplied to the glyoxysome from the mitochondrion.

*siae* (13, 23). In the present work, we used  $^{13}\text{C}$  NMR spectroscopy to examine the flux of carbon originating from exogenous  $[2-^{13}\text{C}]$ acetate into cellular metabolites during acetate adaptation of wild-type *N. crassa* mycelium and correlated the observed distribution of label with the changes in enzymatic activity. In addition, we analyzed two mutants which are unable to grow on acetate. This approach is attractive in that it offers a rapid means of evaluating the metabolic consequences of particular mutations. In addition, it avoids the problems inherent in the assay of unstable enzymes.

## MATERIALS AND METHODS

**Strains and media.** The strains used were obtained from the Fungal Genetics Stock Center, Microbiology Department, University of Kansas Medical School, Kansas City. They were the St. Lawrence 74A wild-type (FGSC 262), *acu-3*(JI38) (FGSC 1732) (10, 11), and *acp*(FS800) (FGSC 3546) strains (24). All were mating type A. Sucrose medium (SM) consisted of Vogel salts (28) plus 1.5% sucrose. Acetate medium (AM) consisted of Vogel salts minus the sodium citrate plus 66 mM sodium acetate. The citrate was omitted to minimize the natural-abundance  $^{13}\text{C}$  NMR signals due to this compound. The final pH of AM and SM was in the range 6.0 to 6.4.  $[2-^{13}\text{C}]$ acetate (90 atom%  $^{13}\text{C}$ ) was obtained from the Prochem Division of British Oxygen Co. Ltd and was substituted for the natural-abundance material in the NMR experiments.

**Growth conditions and transfer from SM to AM.** All growth took place at  $25^\circ\text{C}$ . Initial growth was from conidia inoculated to a density of  $5 \times 10^5/\text{ml}$  in 1.2 liters of SM in a 2-liter conical flask and shaken at 210 rpm. Transfer of log-phase mycelium to AM was done by filtration onto Whatman no. 1 filter paper, brief washing in isothermal distilled water, and suspension in prewarmed AM at a density of 10% (wet weight/volume). Samples (20 to 40 ml) were removed from the cultures at intervals when required, filtered to recover the mycelium, pressed dry, and placed at  $-20^\circ\text{C}$  until lyophilized.

**Enzyme, protein, and amino acid analyses.** Crude extracts for enzyme assays were obtained by extracting the powdered lyophilized mycelium with 10 mM Tris hydrochloride buffer (pH 7.0; 50 ml/g [dry weight]) at ice temperature with intermittent vortexing for 15 to 20 min. The extracts were clarified by centrifugation, and enzyme assays were performed as previously described (11). For amino acid analysis, 20-mg samples of lyophilized mycelium were ground to a

fine powder by vortexing in a 15-ml plastic centrifuge tube in the presence of two steel spatulas. This powder was suspended in 1 ml of 10% sulphosalicylic acid, incubated at ice temperature for 20 to 30 min, and clarified by centrifugation. Amino acid analyses of the resulting supernatants were done with a Beckman IR120 analyzer.

Extracts for NMR analysis were obtained by treating 0.5 to 1.0 g (wet weight) of mycelium with 60% perchloric acid at ice temperature for 10 to 20 min. The mixture was then brought to pH 7.0 with potassium hydroxide, and the salt and cellular debris were removed by centrifugation. The supernatant was freeze-dried and suspended in 20%  $\text{D}_2\text{O}$  in water containing 20  $\mu\text{l}$  of dioxane per ml as an internal standard.

**NMR analysis.** High-resolution  $^{13}\text{C}$  NMR spectra were obtained by using a Bruker WM300 wide-bore spectrometer operating at 75 MHz. The extract spectra were recorded in a 10-mm probe (16,000 time domain data points; acquisition time, 0.54 s; angle,  $30^\circ$ ; time delay, 1.5 s; free induction decays were zero filled to 32,000 before Fourier transformation with a line broadening of 2.0 Hz). High-power broadband decoupling was used during the acquisition, and low power was used during the delays. Spectra of lipid extracts were measured in a 5-mm probe.  $^{13}\text{C}$  chemical shifts were determined by using dioxane as an internal standard at 67.40 ppm. The assignments of resonances in extracts was based on enhancements of the appropriate signals on addition of known concentrations of authentic materials in spectra measured at pH 7.2 and 6.0.  $^1\text{H}$  NMR spectra were obtained on a Bruker WM200 spectrometer at 200 MHz.

$^{13}\text{C}$ -enriched amino acids were isolated from the perchloric acid extracts by cation-exchange chromatography on Bio-Rad AG 50-X2 resin ( $\text{H}^+$  form; 10 by 1 cm) and eluting with a water-1 M pyridine gradient. The ninhydrin-positive fractions were pooled and freeze-dried. The residue was dissolved in water (0.5 ml), adjusted to pH 4 with 2 M HCl, and heated in a sealed tube at  $140^\circ\text{C}$  for 4 h. The resulting mixture was separated by cation-exchange chromatography as described above. Lyophilization of the neutral aqueous eluate yielded L-pyroglutamic acid, formed by the lactamization of the glutamate and glutamine, and the basic eluate contained the remaining unreacted amino acids.  $[^{13}\text{C}]$ alanine was isolated directly from the latter fraction by paper electrophoresis at pH 2.1 (1) on Whatman 3MM filter paper at 300 V/cm. The alanine band was eluted with 0.1 M ammonium hydroxide, and the eluate was freeze-dried. The  $^1\text{H}$  NMR spectra (in  $\text{D}_2\text{O}$ ) of the  $^{13}\text{C}$ -enriched alanine samples exhibited a complex methyl hydrogen signal consisting of a central ( $^{12}\text{CH}_3$ ) doublet ( $^3J_{\text{HH}} = 7.3$  Hz) and a doublet of doublets ( $^{13}\text{CH}_3$ ,  $^3J_{\text{HH}} = 7.3$  Hz,  $^1J_{\text{CH}} = 150$  Hz). In multiply enriched species, both central and satellite signals were split further by  $^{13}\text{C}$  at C-2 ( $^2J_{\text{CCH}} = 4.7$  Hz). Comparison of the integrals for each of these signals allowed the measurement of  $^{13}\text{C}$  enrichment at C-2 and C-3. The enrichment at C-1 was estimated from the normalized intensity of the C-1 resonance compared with those for C-2 and C-3 in the  $^{13}\text{C}$  NMR spectra.

For spectroscopic analysis, samples of the pyroglutamic acid (10 mg) were converted to the anilide by treatment with aniline (15  $\mu\text{l}$ ) and 1-ethyloxycarbonyl-2-ethoxy-1,2-dihydroquinoline (32 mg) in anhydrous dimethylformamide (200  $\mu\text{l}$ ). Removal of the solvent under vacuum and crystallization of the residue from methanol gave pure pyroglutamic acid anilide (mp, 178 to  $182^\circ\text{C}$ ). The  $^{13}\text{C}$  enrichments at the C-2, C-3, and C-4 of the anilide were determined by integration of the  $^{13}\text{C}$  satellites of the corresponding hydrogen

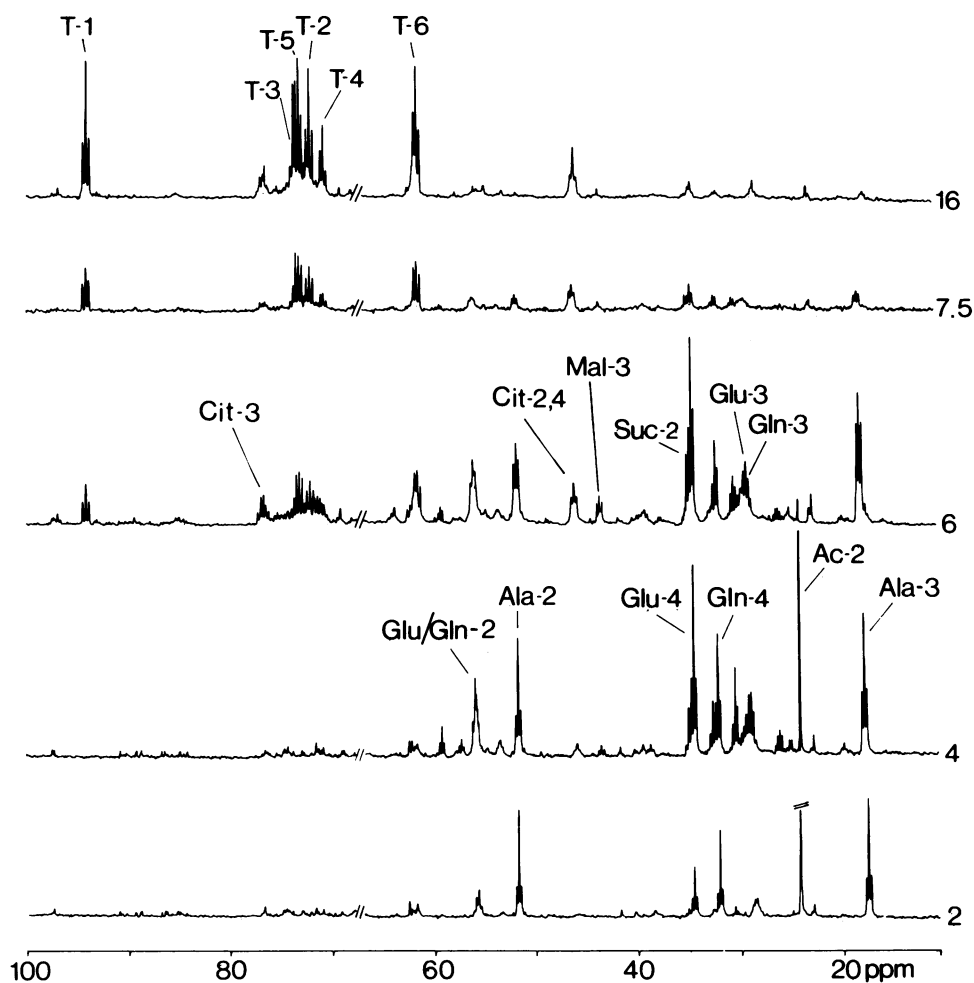


FIG. 2.  $^{13}\text{C}$  NMR spectra of perchloric acid extracts of *N. crassa* mycelium sampled during adaptation to growth on  $[2\text{-}^{13}\text{C}]\text{acetate}$ . The number to the right of each spectrum indicates hours of growth. Intensities are scaled on a dioxane standard at 67.40 ppm (the dioxane peak was omitted for clarity). Each spectrum is the result of 7,000 pulses. Spectra made at 7.5 and 16 h are shown at 0.5 times the vertical scale of the other spectra. T-1 to T-6,  $\alpha,\alpha'$ -trehalose carbons C-1,1' to C-6,6', respectively; Cit-2,4 and Cit-3, C-2, C-4 and C-3 of citrate, respectively; Suc-2, C-2 of succinate; Glu-2, Glu-3, and Glu-4, C-2, C-3, and C-4 of glutamate, respectively; Ala-2 and Ala-3, C-2 and C-3 of alanine, respectively; Mal-3, C-3 of malate. No significant enrichment of carboxyl carbons was observed.

resonances in the  $^1\text{H}$  NMR spectra recorded in  $d_6$ -dimethyl sulfoxide. Enrichments at C-1 were directly measured from the intensity ratios of the  $m/z$  121 and 120 ions [ $(^{13}\text{CO-NHPh})^+$  and  $(^{12}\text{CO-NHPh})^+$ , respectively] in the electron impact mass spectrum of the anilide.

The relative proportions of the  $^{13}\text{C}$ -enriched isotopomers of alanine, glutamate, and glutamine present in different samples were calculated by using the multiplet/singlet ratios measured from  $^{13}\text{C}$  NMR spectra and the  $^{13}\text{C}$  distributions determined by  $^1\text{H}$  NMR and mass spectrometry (8, 21, 22) (see Table 2).

## RESULTS

**Wild-type strain.** The  $^{13}\text{C}$  NMR spectra of a series of perchloric acid extracts of *N. crassa* mycelium made at 1, 2, 4, 6, 7.5, 12, and 16 h after transfer to  $[2\text{-}^{13}\text{C}]\text{acetate}$  medium were measured. Examples are shown in Fig. 2. The earlier spectra, up to 4 h, showed the incorporation of  $^{13}\text{C}$  primarily into alanine, glutamate, and glutamine. Between 4 and 6 h, the signals corresponding to the carbons of trehalose ap-

peared and accumulated. In addition, signals for citrate, malate, and succinate were also evident at this time. From the presence of  $^{13}\text{C}$ - $^{13}\text{C}$  multiplets, it was clear that increasing proportions of multiply enriched species were produced with time. Since the products of the TCA and glyoxylate cycles arise by stereochemically distinct routes, the analysis of labeling patterns in a suitable compound (i.e., of the ratio of different isotopomers present) allowed us to determine the relative predominance of the two cycles. If the TCA cycle was the sole route for the incorporation of the C-2 of acetate into glutamate and glutamine, a 1:1 equilibrium of  $1,2,3,4\text{-}^{13}\text{C}_4$ - and  $2,3,4\text{-}^{13}\text{C}_3$ -labeled species would be predicted (8). In contrast, randomization via the glyoxylate cycle does not permit enrichment of the C-1 position of 2-oxoglutarate, and hence  $[2,3,4\text{-}^{13}\text{C}_3]\text{glutamate}$  and  $[2,3,4\text{-}^{13}\text{C}_3]\text{glutamine}$  accumulate as equilibrium products. Any excess of  $2,3,4\text{-}^{13}\text{C}_3$ -labeled species thus indicates the degree of glyoxylate cycle activity. Determination of the precise proportion of isotopomers for any given species requires knowledge of both the  $^{13}\text{C}$ -multiplet integral ratios obtained from the  $^{13}\text{C}$  NMR spectrum and the  $^{13}\text{C}$  enrichment at each

TABLE 1.  $^{13}\text{C}$ -enrichments and isotopomer ratios for glutamate-glutamine

Time (h) after transfer	$^{13}\text{C}$ atom%				Isotopomer ratio <sup>a</sup>			
	C-1	C-2	C-3	C-4	1,2,3,4- $^{13}\text{C}_4$ <sup>b</sup>	2,3,4- $^{13}\text{C}_3$	2,4- $^{13}\text{C}_2$	4- $^{13}\text{C}$
2	6.7	12.5	15	31	1.0	0.8	<0.2	1.9
4	14	39	36	50	1.0	1.6	0.2	0.8

<sup>a</sup> Relative to the 1,2,3,4- $^{13}\text{C}_4$ -labeled isotopomer.

<sup>b</sup> Includes the 1,3,4- $^{13}\text{C}_3$ -labeled isotopomers.

carbon. The  $^{13}\text{C}$  enrichment at individual carbons of glutamate and glutamine was determined (see Materials and Methods) in extracts made at 2 and 4 h after transfer to AM (Table 1). It is clear that between 2 and 4 h after transfer, the proportion of labeling in the compounds derived via the glyoxylate cycle increased with respect to that derived via the TCA cycle, reaching the relative proportions 0.6:1 (glyoxylate cycle:TCA cycle) by 4 h. This is necessarily a minimum estimate of the final degree of glyoxylate cycle activity since the increase in the activity of its enzymes did not level off until 6 h after transfer under these conditions (Fig. 3; data not shown); the eventual contribution may have been greater.

$^{13}\text{C}$  enrichments determined for the labeled alanine pool are shown in Table 2. The increase in the proportion of [2,3- $^{13}\text{C}_2$ ]alanine with the absence of a detectable 1,2,3- $^{13}\text{C}_3$ -labeled isotopomer is a clear indication of derivation from enriched glyoxylate cycle rather than TCA cycle intermediates. Amino acid analysis of the labeled extracts indicated that there was a threefold increase in the intracellular concentration of free alanine within 30 min of transfer to AM, only a fraction of which was labeled (Fig. 4). Concomitant with this increase was a sharp decline in the size of the glutamate pool. We presume that these changes were linked and occurred because of blockage of a residual glycolytic flux by acetyl-CoA, derived from external acetate, inhibiting pyruvate dehydrogenase (14); the pyruvate accumulated being transaminated to produce alanine, with concomitant deamination of glutamate to 2-oxoglutarate. The alanine aminotransferase (EC 2.6.1.2) necessary for this conversion is known to be present in large quantities (9). Such behavior

is entirely consistent with the previously suggested role of alanine as a store of pyruvate (16).

The apparent lack of any TCA cycle contribution to the labeled alanine pool at times when such a contribution was evident for glutamate-glutamine suggests that the pool was compartmentalized. This is corroborated by the observation that the absolute quantity of labeled material in the pool was constant even during the decline in its overall size (Fig. 4), indicating that the unlabeled material was selectively consumed.

Between 4 and 6 h after the start of incubation in AM, at a time corresponding approximately to the time of induction of maximal PEP carboxykinase activity (Fig. 3), signals corresponding to  $^{13}\text{C}$ -enriched trehalose were seen in the extracts, indicating that gluconeogenesis was occurring (Fig. 2). The rapid synthesis of the disaccharide, enriched principally at C-1, C-2, C-5, and C-6 of the constituent glucose units, was accompanied by a rapid depletion of the [2- $^{13}\text{C}$ ]acetate in the medium (data not shown) and catabolism of the unenriched alanine (Fig. 4). Signals corresponding to the C-3,3' and C-4,4' of  $\alpha,\alpha'$ -trehalose are also evident in the 7.5- and 16-h spectra shown in Fig. 2. The enrichment of these positions, corresponding to labeling at the C-1 of triose phosphate intermediates, indicates a contribution of TCA cycle-randomized oxaloacetate to the gluconeogenic flux.

Examination of the doublet/singlet intensities for trehalose C-1,1', C-6,6', C-2,2', and C-5,5' resonances as a function of time showed that before [2- $^{13}\text{C}$ ]acetate exhaustion the proportion of multiply enriched species increased. As the [2- $^{13}\text{C}$ ]acetate in the medium was consumed,  $^{13}\text{C}$  NMR spectra of lipid extracts of mycelia showed that increasing catabolism of unenriched cellular fatty acid derivatives occurred as exogenous [2- $^{13}\text{C}$ ]acetate was depleted (data not shown). As a result of the progressive dilution of enriched acetyl-CoA, multiple enrichment of intermediates decreased and decreasing multiplet/singlet ratios for the trehalose resonances were observed in the later spectra (Fig. 2). The enhanced singlet nature of the trehalose C-1,1' signal (58%) as opposed to that of the C-6,6' position (41%) is indicative of pentose phosphate pathway cycling of 28% of the gluconeogenically synthesized sugar (8).

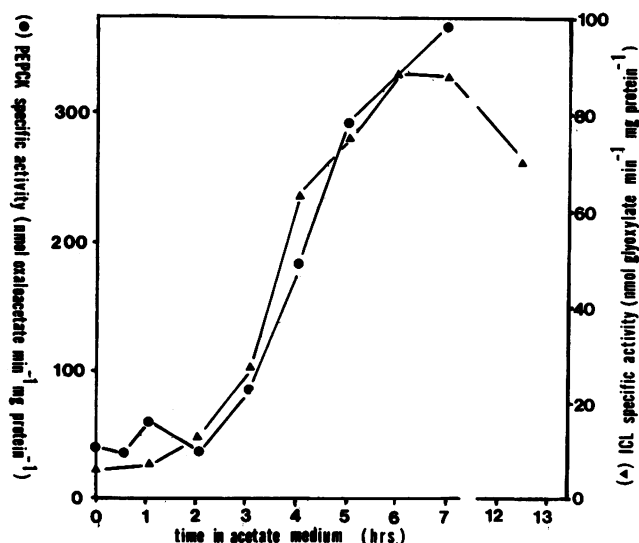


FIG. 3. Increase in specific activity of isocitrate lyase (ICL) and PEP carboxykinase (PEPCK) after transfer to AM under the conditions of the NMR experiments.

TABLE 2.  $^{13}\text{C}$  enrichments and isotopomer ratios for alanine

Time (h) after transfer	$^{13}\text{C}$ atom%			Isotopomer ratio <sup>a</sup>		
	C-1	C-2 <sup>b</sup>	C-3 <sup>c</sup>	2,3- $^{13}\text{C}_2$	2- $^{13}\text{C}$	3- $^{13}\text{C}$
2	ND <sup>d</sup>	12	12	1.2	1.0	0.8
4	ND	24	24	1.6	1.0	0.8
6	ND	50	50	6.4	1.0	1.0
7.5	ND	52	52	7.2	1.0	0.9

<sup>a</sup> Relative to the 2- $^{13}\text{C}$ -labeled isotopomer.

<sup>b</sup>  $^{13}\text{C}$ -enrichments at the C-2 position were estimated from the integrals of the C-3 satellite signals arising from 3-bond coupling of the methyl protons with  $^{13}\text{C}$  at C-2.

<sup>c</sup> Adjusted for the presence of unenriched alanine.

<sup>d</sup> ND, None detectable.

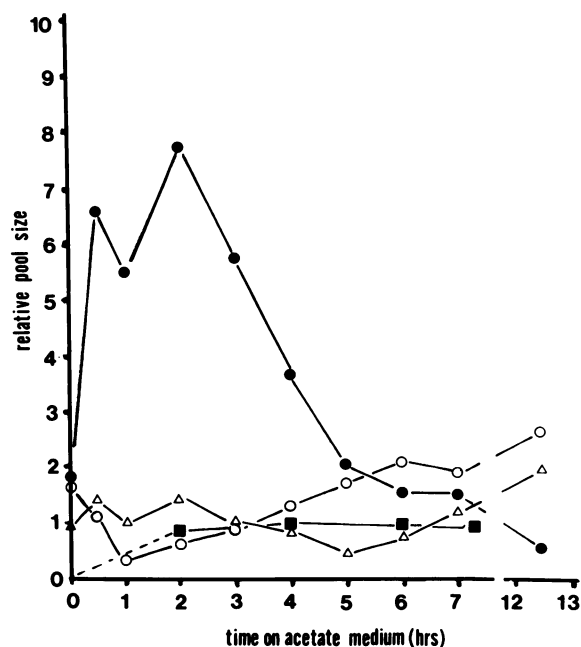


FIG. 4. Amino acid pool sizes, determined as described in Materials and Methods, relative to 150  $\mu$ l of 1 mM norleucine, used as an internal standard. Symbols: ●, alanine; ○, glutamate; △, glutamine; ■,  $^{13}\text{C}$ -enriched alanine calculated by using the pool size at each time and the  $^{13}\text{C}$  enrichments shown in Table 2.

**Acetate metabolism mutants.** We surveyed several mutant strains of *N. crassa* which have an acetate-nonutilizing (*acu*) phenotype (11, 24). Two loci [*acu-3*(JI38) and *acp*(FS800)] appeared "tight," and we describe their characteristics below. However, several of the alleles we examined as representatives of these loci proved to be "leaky" when studied by this methodology [*acu-6*(JI37); *acu-5*(JI18); and *acu-7*(JI36)]; two of these are the sole representatives of these loci held in the Fungal Genetics Stock Center (R. W. Barrat, G. H. Wilson, and R. L. Rimbey, *Neurospora* Newsl. 31:55–141, 1983). This allows some ambiguity in their interpretation, and discussion of their spectra is omitted here. Since no enzyme activity was detected *in vitro* in these strains (11), we presume that the mutated enzymes were unstable under the assay conditions while retaining some activity *in vivo*.

As was done with the wild-type strain, mutant strains were pregrown on SM, transferred to  $2\text{-}^{13}\text{C}$ -labeled AM, and sampled at 2, 6, and 12 h thereafter. The 12-h spectrum for each mutant, along with that of the wild-type strain done in parallel for comparison, is shown in Fig. 5.

(i) *acu-3*(JI38) (an isocitrate lyase-deficient mutant). Mutations at the locus *acu-3* have been assigned unambiguously to the structural gene for the enzyme isocitrate lyase by the analysis of temperature-sensitive mutations (19). The spectrum of the 12-h extract from *acu-3*(JI38) is shown in Fig. 5b and is entirely consistent with the known lesion in isocitrate lyase (19). No gluconeogenesis was evident (indicated by the absence of signals corresponding to trehalose or other sugars), as expected if no anaplerotic flux was possible. There was increased labeling in the C-1 positions of citrate and glutamate (Fig. 5b), consistent with primarily or exclusively TCA cycle randomization of  $[2\text{-}^{13}\text{C}]$ acetate, and there was a very large accumulation of citrate, a putative glyoxysome import substrate (Fig. 1) which would be expected to accu-

multate if an early glyoxylate cycle step was blocked. The accumulation of citrate was so great in fact that it leaked out into the medium (data not shown). Thus, we propose that the intermediate exported from the mitochondrion to the glyoxysome was citrate and that the glyoxysome presumably contained an aconitase (EC 4.2.1.3) activity. Another peculiarity of this mutant, relevant to our interpretation of the wild-type spectra (Fig. 2 and 5a), was the absence of signals corresponding to succinate or malate when the glyoxylate cycle was inoperative, a feature which suggests that these compounds were of anaplerotic origin in the wild-type strain.

(ii) *acp*(FS800) (possibly defective in acetate permease). This mutation has been described as a lesion in an inducible cellular acetate permease presumed to exist alongside its constitutive counterpart (24). Our results (Fig. 5c) demonstrate that acetate readily penetrated the mycelium but that no glyoxylate cycle activity was apparent; a prominent signal corresponding to the C-1 of glutamate indicates primarily or exclusively TCA cycle randomization, and no gluconeogenesis was observed. Thus, if this lesion is indeed in a permease, it must be one that is limited to the glyoxysome. Assays for key enzymes of the glyoxylate cycle and the gluconeogenesis showed them to be present at normal or supranormal levels (Table 3), implying that the *acp* lesion is not a regulatory one which affects the activity of any of these enzymes. A possibility is that the locus is involved in the biogenesis or structural integrity of the glyoxysome itself.

## DISCUSSION

NMR spectra measured with extracts of wild-type mycelium obtained at various times after transfer of the mycelium from medium containing sucrose to that containing  $[2\text{-}^{13}\text{C}]$ acetate as the sole carbon source showed an essentially smooth transition from glycolytic to gluconeogenic metabolism. The label was initially seen in the largest amino acid pools (alanine, glutamate, and glutamine; Fig. 2). Between 2 and 4 h after transfer of the mycelium, the signals corresponding to these amino acids became more complex as coupling with adjacent carbons increased due to the metabolic randomization of precursors via the TCA and glyoxylate cycles.

In all three amino acids,  $^{13}\text{C}$  can only enter the C-1 position from precursors derived by TCA cycling, and this feature allowed us to dissect the contributions of the TCA and glyoxylate cycles in the biosynthesis of these compounds. Analysis of the proportions of isotopomers in the glutamate-glutamine and alanine pools (Tables 1 and 2) indicated that during the period 2 to 4 h after transfer of the mycelium, these amino acid populations became selectively enriched in isotopomers derived from precursors randomized via the glyoxylate cycle. For glutamate-glutamine between 2 and 4 h, the ratio of the contribution of the glyoxylate cycle to that of the TCA cycle to 2-oxoglutarate increased from essentially nil to 0.6:1. Thus, we have evidence for the onset of glyoxylate cycle activity between 2 and 4 h after the transfer to AM. This corresponds well with the increase in the specific activity of the glyoxylate cycle enzyme isocitrate lyase (Fig. 3).

A more dramatic trend was observed for  $^{13}\text{C}$ -enriched alanine; the  $2,3\text{-}^{13}\text{C}_2$ -labeled isotopomer concentration steadily increased in the absence of  $[1,2,3\text{-}^{13}\text{C}_3]$ alanine, indicating an exclusively glyoxylate cycle derivation for this pool. The absence of a TCA cycle contribution to the  $^{13}\text{C}$ -enriched alanine pool suggests that the flux to this amino acid was partitioned in such a way that mitochondrial

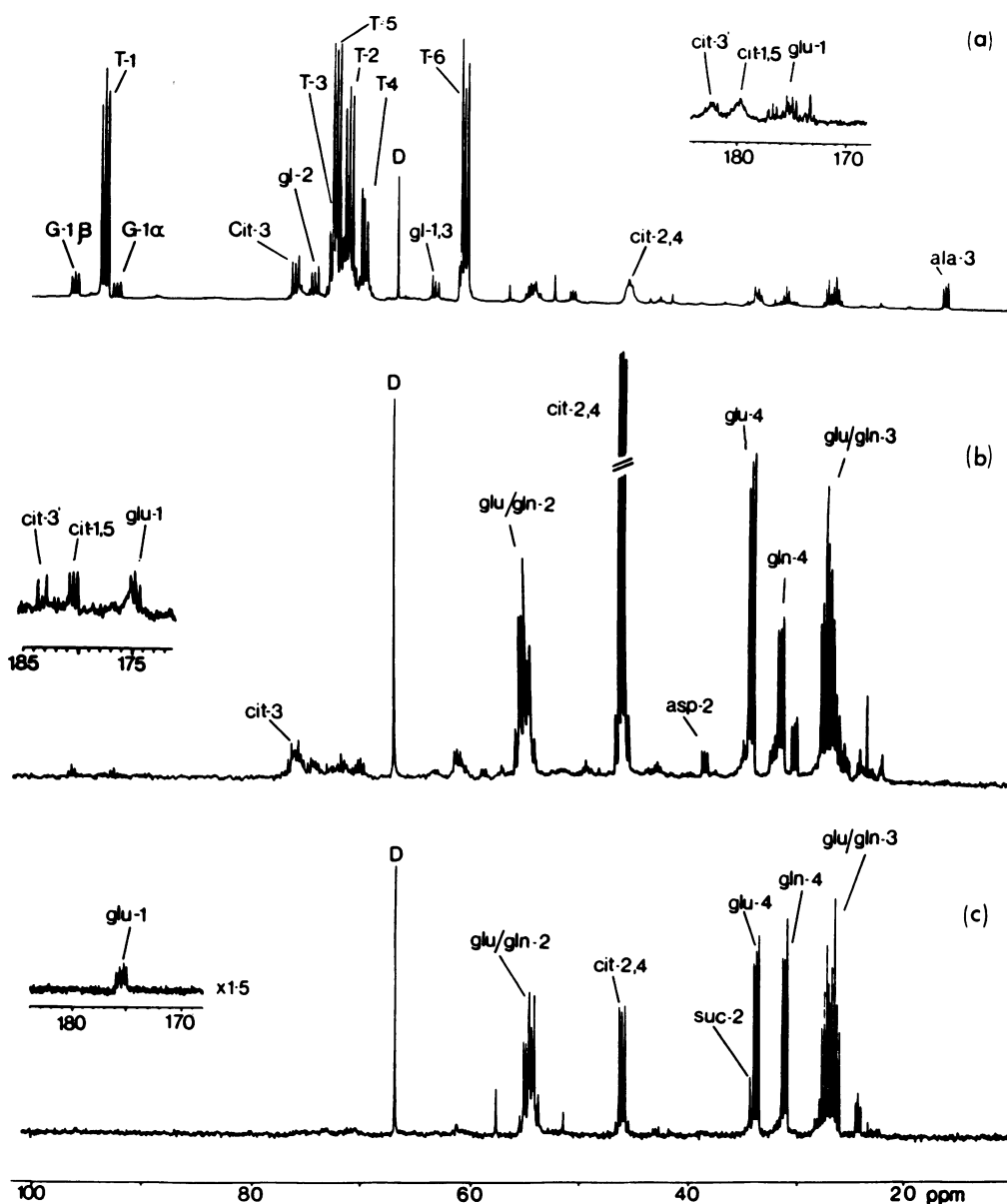


FIG. 5.  $^{13}\text{C}$  NMR spectra of extracts obtained 12 h after transfer to  $2\text{-}^{13}\text{C}$ -labeled AM from wild-type and acetate-nonutilizing strains. (a) Wild-type strain (9,600 pulses); (b) *acu-3* strain (30,000 pulses); (c) *acp* strain (21,000 pulses). The labeling of the peaks is described in the legend to Fig. 2, with the following additions: G-1 $\alpha$  and G-1 $\beta$ , C-1 of  $\alpha$ - and  $\beta$ -glucose, respectively; gl-1,3 and gl-2, C-1, C-3 and C-2 of glycerol, respectively; cit-1,5 and cit-3', C-1, C-5 and C-3' of citrate, respectively; asp-2, C-2 of aspartate; D, dioxane internal standard. The spectra were accumulated as described in Materials and Methods, except for the *acu-3* spectrum, which also contained 5 mM EDTA.

precursors were not used. Amino acid analysis data provide further evidence for the existence of two compartmentally distinct alanine pools. After the transfer to AM, the overall alanine pool size increased dramatically (Fig. 4), but only a small proportion of molecules in the pool were enriched in  $^{13}\text{C}$ . When this pool declined 2 h after transfer, only the unenriched alanine was consumed; the simplest explanation for this is compartmentalization of the  $^{13}\text{C}$ -enriched material such that it was not subject to this drain.

Alanine has not been reported to be sequestered, other than in the cytosol, in *N. crassa*. Direct isolation of vacuoles (27) has shown that less than 1% lies in this organelle, and only about 6% is present in other organelles. Similarly, in vivo experiments using  $^{15}\text{N}$  NMR have demonstrated that

the bulk of the alanine lies in an environment different in both pH (20) and viscosity (15) from that of vacuolar amino acids such as arginine and histidine. However, by the time the alanine pool was restored to its initial level (Fig. 4), the  $^{13}\text{C}$ -enriched pool was 50% of the cellular alanine. That this degree of compartmentalization of the alanine pool preexisted on SM appears unlikely (15, 20, 27), suggesting that the sequestration increased as part of the adaptation process. Given that the unenriched alanine pool and gluconeogenesis were cytosolic and that there was evidence for a TCA cycle contribution to the latter in the  $^{13}\text{C}$  enrichments of C-3,3' and C-4,4' of trehalose (Fig. 2), whereas the  $^{13}\text{C}$ -enriched alanine pool showed no such contribution (Table 2), we are led to two related possibilities for the identity of the compartment

TABLE 3. Specific enzyme activities in wild-type and *acp*(FS800) mycelium at various times after transfer from SM to AM

Strain	Time (h) after transfer	Sp act ( $\mu\text{mol}$ of product/min per mg of protein) of <sup>a</sup> :		
		ICL	MS	PEPCK
Wild type	0	0.001	0.003	0.002
	6	0.084	0.097	0.921
	12	0.070	0.108	0.988
<i>acp</i>	0	ND	ND	ND
	6	0.202	0.179	0.889
	12	0.252	0.241	0.152

<sup>a</sup> ICL, Isocitrate lyase; MS, malate synthase; PEPCK, PEP carboxykinase; ND, not determined.

containing the <sup>13</sup>C-enriched alanine. Either it is the glyoxysome itself or it is directly derived from glyoxysomal intermediates by some tightly channeled transport process which does not permit dilution from the cytosol.

Between 4 and 6 h after the transfer to AM, as the alanine pool neared its basal level and the induced enzymes approached their maximum specific activities (Fig. 3), labeling of the disaccharide trehalose was observed (Fig. 2). There was a detectable increase in the specific activity of PEP carboxykinase between 2 and 3 h after the transfer (Fig. 3), and it is probable that gluconeogenesis occurred earlier than the observation of label in trehalose suggests. For this to be the case, unenriched precursors must have been utilized, and it is likely that the accumulated (unenriched) alanine provided the source for these precursors. The large size of this pool would necessarily have diluted out the enriched precursors, and its decline commenced in parallel with the increase in the induced enzyme activities (Fig. 3 and 4). In later spectra, between 7.5 and 16 h, a decline in the degree of coupling in the trehalose carbons was observed which can be correlated with exhaustion of exogenous [<sup>2-13</sup>C]acetate and catabolism of stored lipids.

Our principal aim in studying the acetate-nonutilizing mutants was to characterize their metabolic defects based on the flux of labeled precursor into cellular metabolites and hence to clarify the nature and extent of specific lesions. Additionally, knowledge of the metabolism of these strains should enhance our understanding of the sequence of events involved in acetate adaptation in the wild-type strain.

Except for the *acp*(FS800) mutation, our results are entirely consistent with the previously assigned or suspected lesions, although a surprising number of the mutants were found to be leaky [*acu-6*(JI37), *acu-5*(JI18), and *acu-7*(JI36); data not shown] despite the reported absence of detectable enzyme activity in vitro (11). Since low levels of activity (relative to that in the wild-type strain) may be all that is required to produce a substantial flux through a pathway (17), then only a low level of enzyme activity, allowing a detectable flux in vivo, need go undetected in an in vitro assay. Moreover, an unstable mutant enzyme might not survive the rigors of extraction and in vitro assay. However, it should be emphasized that the phenotype of these mutants is severe in that they cannot grow on acetate as the sole carbon source (10, 24), and it is perhaps a more pleiotropic effect of the mutations rather than the immediate decrease in flux in that step which causes the phenotype.

The two mutant strains which we examined that could be described as carrying tight mutations were *acu-3*(JI38) and *acp*(FS800). The *acu-3*(JI38) mutation is known to lie in the structural gene for isocitrate lyase (19), and the NMR data

are entirely consistent with this. The *acu-3*(JI38) strain carried out no detectable gluconeogenesis, consistent with an inactive anaplerotic pathway (i.e., the glyoxylate cycle) and accumulated large quantities of citrate, the immediate precursor of isocitrate, the substrate of the inactive enzyme. Why citrate accumulated rather than isocitrate is unclear; however, the accumulation of citrate as opposed to its oxidation via the TCA cycle suggests that it was exported from the mitochondrion and leads us to favor pathway 1 in Fig. 1 as the connection between this organelle and the glyoxysome. This indicates that there should be an aconitase activity associated with the latter, which has not been demonstrated.

It has been suggested (26) that there is an isozyme of isocitrate lyase present in *N. crassa*. However, a second report suggested that this might be an artifact (A. Rougemont and M. J. Kobr, *Neurospora* Newsl. 20:28-29, 1973). Our results with the *acu-3*(JI38) lesion support the latter contention since this mutation seems to abolish glyoxylate cycle activity completely.

The *acp*(FS800) mutation was first described as a lesion in an inducible acetate transport system (24). Although we did not show that such a system does not exist, the data suggest that this mutation affects some other function. The NMR spectra measured with extracts of this strain indicate that it does not possess an operational glyoxylate cycle, since randomization of the label occurred from TCA cycle activity and no gluconeogenesis could be detected. Assays for the enzymes isocitrate lyase, malate synthase, and PEP carboxykinase indicated that they were present at normal levels, which leaves the true nature of the mutation uncertain. Three likely possibilities are as follows. First, the mutation may affect some other enzyme activity not assayed in this study. However, complementation tests (24) have indicated that *acp*(FS800) is not allelic to *acu-3*, *-5*, *-6*, or *-7*, which leaves only the putative aconitase activity as a possibility for a glyoxysome-specific enzymatic lesion. However, if this is the case, we would expect citrate exported from the mitochondrion to accumulate, as is the case with the *acu-3*(JI38) strain. The second possibility is that the *acp*(FS800) mutant is defective in some kind of transport function between organelles, such as the putative mitochondrial citrate export function (the citrate would then be oxidized instead of accumulating) or an acetate permease specific to the glyoxysome. Third, since it is thought that the glyoxysome is a distinct subclass of catalase-negative microbodies in *N. crassa* (7, 29), the *acp* gene could be involved in the biogenesis or structural integrity of this organelle.

The reason for the probable misinterpretation of the *acp* mutation lies in the inducible nature of the acetate-utilizing enzymes. In the original description of this strain (24), the acetate taken up by wild-type conidia was shown to remain largely as acetate over a period of 60 min, and a preincubation of 180 min in 1 mM acetate was required for maximal stimulation of the "inducible permease." It is clear from our data (Fig. 2) that after this period of time, acetate had been metabolized to other intermediates. Thus, it is likely that the increased uptake of [<sup>14</sup>C]acetate induced by this treatment (24) was most probably due to the induction of an acetate sink, i.e., the glyoxylate cycle and gluconeogenesis. It is this sink which is clearly lacking in the *acp* strain.

Some genes are regulated transcriptionally during acetate adaptation (G. H. Thomas, Ph.D. thesis, University of Edinburgh, Edinburgh, United Kingdom, 1984), and based on inhibitor studies, it is likely that this includes the enzyme activities of the glyoxylate cycle and gluconeogenesis which

increase at this time (R. B. Flavell, Ph.D. thesis, University of Leeds, Leeds, United Kingdom, 1967). Therefore, it is important that the regulatory effector(s) in this process be identified. A more detailed understanding of the biochemistry of the adaptation process should indicate the areas of metabolism which should be examined to identify these molecules. We showed that  $^{13}\text{C}$  NMR is a useful tool with which to probe this biochemical system.

#### ACKNOWLEDGMENTS

We thank R. A. Ambler and his staff for amino acid analyses.

We acknowledge financial support from the Science and Engineering Research Council. G.H.T. was supported by a Medical Research Council Studentship in the laboratory of J. R. S. Fincham.

#### LITERATURE CITED

1. Ambler, R. P. 1963. The amino acid sequence of *Pseudomonas* cytochrome C-551. *Biochem. J.* **89**:349-378.
2. Baxter, R. L. 1985. Microbiological applications of NMR spectroscopy. *Microbiol. Sci.* **2**:340-345.
3. Baxter, R. L., N. E. Mackenzie, and A. I. Scott. 1983. CMR as a probe for metabolic pathways *in vivo*. *Biol. Magn. Reson.* **5**:1-20.
4. Breidenbach, R. W., and H. Beevers. 1967. Association of the glyoxylate cycle enzymes in a novel subcellular particle from castor bean endosperm. *Biochem. Biophys. Res. Commun.* **27**:462-469.
5. Cioni, M., G. Pinzauti, and P. Vanni. 1981. Comparative biochemistry of the glyoxylate cycle. *Comp. Biochem. Physiol.* **70B**:1-26.
6. denHollander, J. A., K. L. Behar, and R. G. Schulman. 1981.  $^{13}\text{C}$ -NMR study of transamination during acetate utilization by *Saccharomyces cerevisiae*. *Proc. Natl. Acad. Sci. USA* **78**:2693-2697.
7. Desel, H., R. Zimmermann, M. Janes, F. Miller, and W. Neupert. 1982. Biosynthesis of glyoxysomal enzymes in *Neurospora crassa*. *Ann. N.Y. Acad. Sci.* **386**:377-388.
8. Dickinson, J. R., I. W. Dawes, A. J. Boyd, and R. L. Baxter. 1983.  $^{13}\text{C}$ -NMR studies of acetate metabolism during sporulation of *Saccharomyces cerevisiae*. *Proc. Natl. Acad. Sci. USA* **80**:5847-5851.
9. Fincham, J. R. S. 1951. Transaminases in *Neurospora crassa*. *Nature (London)* **168**:957-958.
10. Flavell, R. B., and J. R. S. Fincham. 1968. Acetate-nonutilizing mutants of *Neurospora crassa*. I. Mutant isolation, complementation studies, and linkage relationships. *J. Bacteriol.* **95**:1056-1062.
11. Flavell, R. B., and J. R. S. Fincham. 1968. Acetate-nonutilizing mutants of *Neurospora crassa*. II. Biochemical deficiencies and the roles of certain enzymes. *J. Bacteriol.* **95**:1063-1068.
12. Flavell, R. B., and D. O. Woodward. 1970. The concurrent regulation of metabolically related enzymes. *Eur. J. Biochem.* **17**:284-291.
13. Gilles, R. J., and A. G. Benoit. 1983. Analysis of a cell division mutant of *Saccharomyces cerevisiae*. *Biochim. Biophys. Acta* **762**:466-470.
14. Harding, R. W., D. F. Caroline, and R. P. Wagner. 1970. The pyruvate dehydrogenase complex from the mitochondrial fraction of *Neurospora crassa*. *Arch. Biochem. Biophys.* **138**:653-661.
15. Kanamori, K., T. L. Legerton, R. L. Weiss, and J. D. Roberts. 1982. Nitrogen-15 spin-lattice relaxation times of amino acids in *Neurospora crassa* as a probe of intracellular environment. *Biochemistry* **21**:4916-4920.
16. Kanamori, K., T. L. Legerton, R. L. Weiss, and J. D. Roberts. 1982. Effect of nitrogen source on glutamine and alanine biosynthesis in *Neurospora crassa*. *J. Biol. Chem.* **257**:14168-14172.
17. Kascser, H., and J. A. Burns. 1979. Molecular democracy: who shares the controls? *Biochem. Soc. Trans.* **7**:1149-1160.
18. Kobr, M. J., F. Vanderheagh, and G. Combepine. 1969. Particulate enzymes of the glyoxylate cycle in *Neurospora crassa*. *Biochem. Biophys. Res. Commun.* **37**:640-645.
19. Leckie, B. J., and J. R. S. Fincham. 1971. A structural gene for *Neurospora crassa* isocitrate lyase. *J. Gen. Microbiol.* **65**:35-43.
20. Legerton, T. L., K. Kanamori, R. L. Weiss, and J. D. Roberts. 1983. Measurements of cytoplasmic and vacuolar pH in *Neurospora* using nitrogen-15 nuclear magnetic resonance spectroscopy. *Biochemistry* **22**:899-903.
21. London, R. E., V. H. Killman, and N. A. Matwiyoff. 1975. The quantitative analysis of carbon-carbon coupling of the molecules synthesized from  $^{13}\text{C}$ -enriched precursors. *J. Am. Chem. Soc.* **97**:3565-3573.
22. Matwiyoff, N. A. 1982.  $^{13}\text{C}$  nuclear magnetic resonance studies of the biosynthesis by *Microbacterium ammoniaphylum* of L-glutamate selectively enriched with carbon-13. *J. Biol. Chem.* **257**:1189-1195.
23. Navon, G., R. G. Schulman, T. Yamane, T. R. Eccleshall, K. B. Lam, J. J. Baronofsky, and J. Marmur. 1979. Phosphorus-31 nuclear magnetic resonance studies of wild type and glycolytic pathway mutants of *Saccharomyces cerevisiae*. *Biochemistry* **18**:4487-4499.
24. Rao, T. K., and A. G. DeBusk. 1977. An inducible acetate transport system in *Neurospora crassa* conidia. *Biochim. Biophys. Acta* **470**:475-483.
25. Schwitzguebel, J. P., M. Moller, and J. M. Palmer. 1981. Changes in density of mitochondria and glyoxysomes from *Neurospora crassa*: a re-evaluation utilizing silica sol gradient centrifugation. *J. Gen. Microbiol.* **126**:289-295.
26. Sjorgren, R. E., and A. H. Romano. 1967. Evidence for multiple forms of isocitrate lyase in *Neurospora crassa*. *J. Bacteriol.* **93**:1638-1643.
27. Vaughn, L. E., and R. H. Davis. 1981. Purification of vacuoles from *Neurospora crassa*. *Mol. Cell. Biol.* **1**:797-806.
28. Vogel, H. J. 1964. Distribution of lysine pathways among fungi: evolutionary implications. *Am. Nat.* **98**:435-446.
29. Wanner, G., and R. R. Theimer. 1982. Two types of microbodies in *Neurospora crassa*. *Ann. N.Y. Acad. Sci.* **386**:269-282.